

Enhancement of the High-Rate Capability of Solid-State Lithium Batteries by Nanoscale Interfacial Modification**

By Narumi Ohta, Kazunori Takada,* Lianqi Zhang, Renzhi Ma, Minoru Osada, and Takayoshi Sasaki

Rechargeable lithium batteries are widely used in portable equipment today.^[1] However, there have always been safety issues arising from their combustible organic electrolytes. These issues are becoming more serious with the increasing size of batteries for use in electric vehicle (EV) or load-leveling applications. Nonflammable solid electrolytes would be the ultimate solution to the safety issue. Despite their high safety, the energy densities and power densities of solid systems have been too low for their practical use. We have succeeded in increasing their energy densities to levels comparable to those of liquid ones.^[2,3] However, power densities, or high-rate capabilities, remain poor. In this communication, we report that a buffer film with a thickness of only several nanometers interposed between the electrode and electrolyte materials improves the high-rate capability of solid-state lithium batteries.

Low ionic conductivities of solid electrolytes have been the reason for the poor high-rate capability of solid-state lithium batteries. Although the conductivities of recently discovered solid electrolytes^[4,5] ($> 10^{-3} \text{ S cm}^{-1}$) are slightly lower than those observed for liquid electrolytes, Li^+ ionic conduction in the solid electrolytes has become as fast as that of liquid electrolytes, by taking into account the fact that the transport number of ions in inorganic electrolytes is unity. However, the high-rate capability of solid systems, including solid electrolytes, remains inferior.

This fact strongly suggests that the rate-controlling step is not in the bulk of the solid electrolytes, but at the interface between the electrode and the electrolyte materials.

Ionic conduction at interfaces between different kinds of ionic conductors, or heterojunctions, is characterized by the term “nanoionics”;^[6] a frontier study was done for a $\text{LiI-Al}_2\text{O}_3$ composite,^[7] and a sophisticated example was presented by Sata et al.^[8] In the latter, two kinds of F^- ion conductors, BaF_2 and CaF_2 , were brought into contact with each other. Part of the F^- ions then transferred from one side to the other to reach an equilibrium, which produced vacancies in the former and interstitial ions in the latter, both of which contributed to ionic conduction at the interface and enhanced the ionic conduction. Similar nanoionic phenomena should take place at the interface between the electrode and the electrolyte materials, forming a space-charge layer. Because the compositions and structures of solid electrolytes have been well tailored to achieve high ionic conductivities, the ionic conductivity of the space-charge layer, where the compositions deviate from the optima, should be lower than that of the bulk, increasing the interfacial resistance. For instance, the $\text{Li}_4\text{GeS}_4\text{-Li}_3\text{PS}_4$ (thio-LISICON) system used in the present study has a high ionic conductivity of the order of $10^{-3} \text{ S cm}^{-1}$ at its optimum composition. However, variation in the composition reduces it to $10^{-6} \text{ S cm}^{-1}$.^[4]

The detrimental increase in the interfacial resistance would be prominent in bulk-type or non-thin-film solid-state lithium batteries. Sulfide electrolytes should be used in such batteries, because the ionic conductivities of oxide solid electrolytes, for example, are so low that they are available only in thin-film systems.^[9] On the other hand, the cathode should be an oxide, such as LiCoO_2 , because of its high electrode potential.^[10,11] When the sulfide electrolytes are in contact with the oxide electrodes, the large difference between their chemical potentials should make Li^+ ions transfer from the sulfide electrolytes to the oxide electrodes. In addition, such a space-charge layer in the sulfide electrolyte would be much more developed when in contact with a mixed-conducting oxide, such as LiCoO_2 , rather than an ion-conducting oxide. When an ion-conducting sulfide is in contact with an ion-conducting oxide, the transfer of Li^+ ions forms space-charge layers not only in the sulfide but also in the oxide. When the oxide also has electronic conduction, that is, it is a mixed conductor, the space-charge layer on the oxide side of the interface should vanish, because the electronic conduction resolves the concentration gradient of the Li^+ ions. Consequently, Li^+ ions should additionally transfer from the sulfide in order to reach an equilib-

[*] Dr. K. Takada, Dr. N. Ohta,^[†] Dr. L. Zhang, Dr. R. Ma, Dr. M. Osada, Dr. T. Sasaki
Advanced Materials Laboratory
National Institute for Materials Science
1-1 Namiki, Tsukuba, Ibaraki 305-0044 (Japan)
E-mail: takada.kazunori@nims.go.jp

Dr. K. Takada, Dr. T. Sasaki
Core Research for Evolutional Science and Technology (CREST)
Japan Science and Technology Agency (JST)
4-1-8 Honcho, Kawaguchi, Saitama 332-0012 (Japan)

[†] Present address: Polymer Electrolyte Fuel Cell Cutting-Edge Research Center, National Institute of Advanced Industrial Science and Technology (AIST), 2-41-6 Aomi, Koto-ku, Tokyo 135-0064, Japan.

[**] We thank T. Kurihara of Powrex Corp. for his help in the preparation of the coated LiCoO_2 , and Y. Kobayashi and A. Yamanaka of the Central Research Institute of Electric Power Industry for their suggestions in the coating experiment. We also thank S. Takenouchi of our institute for the ICP-AES. This work was partially funded by the Ministry of Economy, Trade and Industry (METI) and New Energy and Industrial Technology Development Organization (NEDO). Supporting Information is available online from Wiley InterScience or from the author.

rium, further developing the space-charge layer on the sulfide side and resulting in a very large interfacial resistance.

The above scenario has led us to a strategy to suppress the development of a space-charge layer in the sulfide electrolyte in order to decrease the resistance and improve the high-rate capability of solid-state lithium batteries: an additional thin film of an ion-conducting and electron-insulating oxide should be interposed between the oxide electrode and the sulfide electrolyte. The interposition forms two interfaces: one between the mixed-conducting oxide electrode and the ion-conducting oxide, and another between the ion-conducting oxide and the sulfide. The space-charge layers at both interfaces will be less developed, because the former consists of oxides with similar chemical potentials, and the latter consists of electron-insulating materials. Therefore, a 3d transition metal oxide, $\text{Li}_4\text{Ti}_5\text{O}_{12}$,^[12] was chosen for the interposing layer between the oxide electrode (LiCoO_2) and the sulfide electrolyte (thio-LISICON). Of course, $\text{Li}_4\text{Ti}_5\text{O}_{12}$ is well known as an electrode material. Li^+ ions are reversibly inserted into it, which brings about electronic conduction. However, the insertion takes place at potentials lower than 1.5 V.^[12] Li^+ ions should not be inserted in the $\text{Li}_4\text{Ti}_5\text{O}_{12}$ layer when it is on the 4 V cathodes; thus, it should act as an electron-insulating layer.

We coated the surface of the LiCoO_2 with $\text{Li}_4\text{Ti}_5\text{O}_{12}$ by spray-coating. Seven samples with different coating thicknesses were prepared, and they were labeled by the thickness; that is, the coating layer of sample 5 had an average thickness of ca. 5 nm. Their electrode properties were investigated in solid-state electrochemical cells as described in the Experimental section. Electrochemical impedance spectroscopy (EIS) clearly demonstrated the reduction of the interfacial resistance by the interposition of $\text{Li}_4\text{Ti}_5\text{O}_{12}$ (Fig. 1). Each spectrum consisted of a semicircle in the high-frequency region (>0.5 Hz), which was assigned to the interfacial response, followed by a straight line in the lower-frequency region (<0.5 Hz) corresponding to a Warburg impedance. The high-frequency limits were almost constant, which were attributable to the resistances of the electrolyte layers. Changing the thickness of the coating layer changed the diameter of the semicircle, i.e., the interfacial resistance. The minimum resistance (44 Ω) was observed for sample 5, which was 20 times smaller than that for uncoated LiCoO_2 (910 Ω).

High-rate capability was improved as the interfacial resistance was decreased. Figure 2 shows the discharge curves at various discharge rates. The discharge capacity was increased by the coating, and again, the best performance was observed for sample 5. For example, 64 % of the capacity was retained at 5 mA cm^{-2} for sample 5, whereas only 4 % of the capacity was retained for the uncoated sample. The coated LiCoO_2 gave a discharge capacity of 44 mA h g^{-1} even at a high current density of 10 mA cm^{-2} (0.88 A g^{-1}), which is the highest current drain for inorganic solid-electrolyte batteries reported so far.

The suppression of the formation of the highly resistive space-charge layer by the interposition of the $\text{Li}_4\text{Ti}_5\text{O}_{12}$ layer

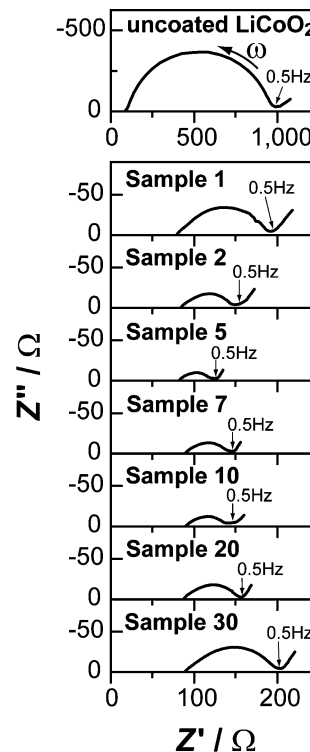


Figure 1. Complex impedance (Z) plots of the In-Li/ LiCoO_2 cells.

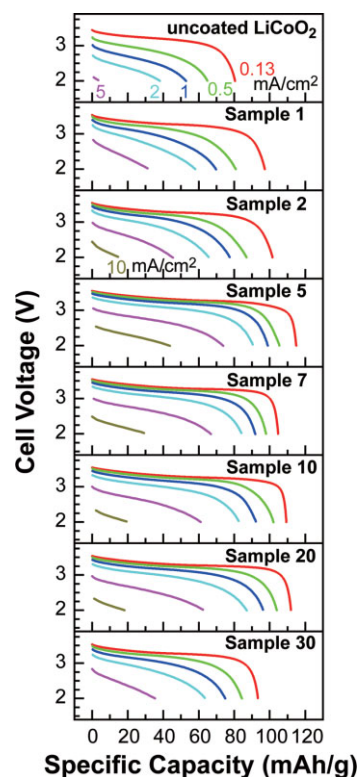


Figure 2. Discharge curves of the In-Li/ LiCoO_2 cells. The horizontal axes indicate the specific capacity calculated on the basis of the weight of the uncoated or coated LiCoO_2 .

was clearly recognized at the beginning of the first charge curves shown in Figure 3. The space-charge layer is considered to be developed by the transfer of Li^+ ions from the solid electrolyte to LiCoO_2 . The introduced Li^+ ions are deinterca-

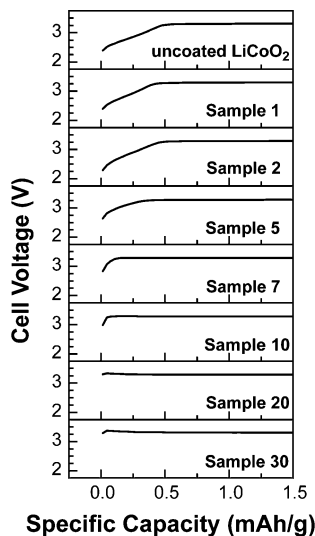


Figure 3. Charge curves of the In-Li/ LiCoO_2 cells at the beginning of the first charge.

lated prior to those originally accommodated in the LiCoO_2 , giving an additional step in the beginning of the first charging process. In fact, the charge curve for uncoated LiCoO_2 showed a slope prior to a plateau at 3.3 V.

The slope faded as the thickness of the $\text{Li}_4\text{Ti}_5\text{O}_{12}$ coating increased, strongly supporting the idea that the $\text{Li}_4\text{Ti}_5\text{O}_{12}$ layer covering the surface of the LiCoO_2 particles suppressed the Li^+ ion transfer and the resultant formation of the space-charge layer. When the dose increased further, the slope completely disappeared; however, the high-rate capability deteriorated, which can be ascribed to the low ionic conductivity of $\text{Li}_4\text{Ti}_5\text{O}_{12}$.^[13] That is, the resistance of the coating layer itself controlled the current drain.

The improvement of power density by the coating was evaluated in a solid-state “lithium-ion” cell; that is, graphite was used in place of the In-Li alloy in order to make a comparison with commercialized lithium-ion cells. Figure 4 shows the discharge curves at various current densities and the relationship between the energy density and the average power density (Ragone plot^[14]). Because the charge-transfer process in the cathode had been the rate-controlling step, the coated LiCoO_2 cathode markedly enhanced the high-rate capability. Although the weights of the electrolyte layer and the battery case are excluded in the calculation of the energy and power densities, they are clearly comparable to commercialized lithium-ion cells.^[15,16]

In summary, the high-rate capability of a solid-state lithium battery with sulfide electrolytes was significantly improved when the LiCoO_2 particles were coated with $\text{Li}_4\text{Ti}_5\text{O}_{12}$. The

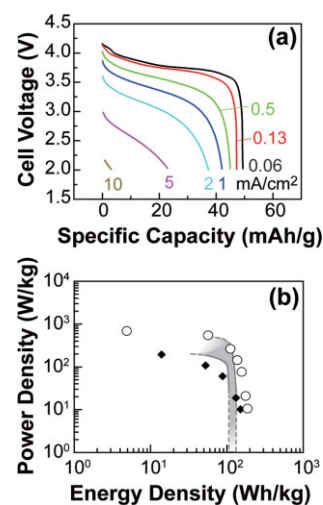


Figure 4. High-rate capability of C/ LiCoO_2 batteries. a) Discharge curves of the battery at various current densities. The horizontal axis indicates the specific capacity that was calculated on the basis of the weight of both the cathode and anode mixtures (12.7 mg+5.1 mg). b) Ragone plots. The plots for the present battery with the coated LiCoO_2 (○) were derived from the discharge curves in (a). Data for the batteries with the uncoated LiCoO_2 (◆) are also plotted. The shaded area indicates energy and power densities of commercialized lithium-ion batteries reported in the literature [16].

power densities observed in the solid-state battery with the coated LiCoO_2 were comparable to commercialized lithium-ion cells. We believe that the enhancement of the high-rate capability will pave the way for the practical application of solid-state lithium batteries and, hence, provide a solution to the safety concerns of lithium batteries.

Experimental

Preparation and Characterization of LiCoO_2 Coated with $\text{Li}_4\text{Ti}_5\text{O}_{12}$: Commercial LiCoO_2 powder (D10, Toda Kogyo; average particle size of 11.2 μm and Brunauer–Emmett–Teller (BET) surface area of 0.26 m^2g^{-1}) was used for the preparation. The $\text{Li}_4\text{Ti}_5\text{O}_{12}$ coating layer was formed from an ethanol solution of alkoxides of lithium and titanium. Under an Ar atmosphere, 4.1 g (0.59 mol) of lithium metal (Honjo Chemical) was dissolved in 487.0 g of dry ethanol (Kanto Chemical) and mixed with 208.9 g (0.74 mol) of titanium tetraisopropoxide (Kanto Chemical). The solution was sprayed onto the LiCoO_2 powder (1.5 kg) at a spraying rate of 2 g min^{-1} by a rolling fluidized coating machine (MP-01, Powrex). During the coating process, seven coated samples were taken from the fluidized bed when certain amounts of the solution were applied. The coated samples and the uncoated LiCoO_2 reference sample were finally heated at 400 °C for 30 min under an oxygen flow to obtain $\text{Li}_4\text{Ti}_5\text{O}_{12}$ -coated LiCoO_2 .

The fraction of $\text{Li}_4\text{Ti}_5\text{O}_{12}$ in the coated samples was determined from the contents of Co and Ti, analyzed by inductively coupled plasma–atomic emission spectroscopy (ICP–AES). Table 1 lists the gravimetric fractions of the $\text{Li}_4\text{Ti}_5\text{O}_{12}$ calculated from the doses of the alkoxide solution and deduced from the ICP results. The average thicknesses of the coating layers were in accordance with the values expected from the amounts of the applied solutions. However, they gradually became thicker than the expected values. Because the blast from the fluidization discharged some of the LiCoO_2 powder during the coating process, the deviation became larger when the thicker coating layers were formed.

Table 1. Gravimetric fractions and thickness of $\text{Li}_4\text{Ti}_5\text{O}_{12}$ layer.

Sample No.	1	2	5	7	10	20	30
Doses of the alkoxide solution [g]	14	28	70	98	140	280	420
Calculated fractions of $\text{Li}_4\text{Ti}_5\text{O}_{12}$ [wt %]	0.09	0.18	0.44	0.62	0.89	1.76	2.61
Analytical fractions of $\text{Li}_4\text{Ti}_5\text{O}_{12}$ [wt %]	0.09	0.18	0.47	0.66	0.97	2.08	3.36
Calculated thickness of $\text{Li}_4\text{Ti}_5\text{O}_{12}$ [nm]	1	2	5	7	10	20	30
Analytical thickness of $\text{Li}_4\text{Ti}_5\text{O}_{12}$ [nm]	1.1	2.2	5.4	7.8	11.3	24.8	38.9

The X-ray diffraction patterns for the samples indicated that the crystal structure of LiCoO_2 [17] remained unchanged, and the Raman spectra from the coating layer were similar to that of $\text{Li}_4\text{Ti}_5\text{O}_{12}$ with spinel structure [18]. The scanning and transmission electron microscopy observations and the energy dispersive X-ray (EDX) analysis of the surface of the powder (see Supporting Information) revealed that the $\text{Li}_4\text{Ti}_5\text{O}_{12}$ was distributed evenly over the surface of the LiCoO_2 particles.

Electrochemical Measurements: Two kinds of sulfide electrolytes, $\text{Li}_{3.25}\text{Ge}_{0.25}\text{P}_{0.75}\text{S}_4$ (thio-LISICON) [4] and $70\text{Li}_2\text{S}-30\text{P}_2\text{S}_5$ glass ceramic [5], were used for the electrochemical measurements; the former was synthesized by a modified literature procedure [4], and the latter was kindly supplied by Idemitsu Kosan Co., Ltd.

Solid-state electrochemical cells to investigate the high-rate capability of the coated LiCoO_2 were fabricated with the thio-LISICON as the solid electrolyte and In–Li alloy as the counter electrode. In–Li alloy shows a flat potential plateau (0.62 V vs. Li/Li^+) and a large exchange current density [19], and thus it is suitable for electrochemical measurements. The positive electrode was a mixture of LiCoO_2 (coated or uncoated) and thio-LISICON at a weight ratio of 7:3. The cathode mixture (12.7 mg), ground electrolyte powder (150 mg), and the In–Li alloy, formed by attaching a small piece of lithium foil (<1 mg) to an indium foil (60 mg), were pressed together at 500 MPa into a three-layer 1 cm diameter pellet.

The cells and the batteries were charged and discharged in galvanostatic mode at room temperature using a multi-channel galvanostat (PS-08, Toho Giken). They were charged to 3.58 V at $127.4 \mu\text{A cm}^{-2}$ and then discharged down to 2 V at various current densities. Electrochemical impedance spectroscopy (EIS) was performed for the cells. After the cells were charged to 3.58 V at $127.4 \mu\text{A cm}^{-2}$ followed by a rest period of 30 min, the impedance spectra were recorded by using a frequency response analyzer (1260, Solartron Analytical) coupled with an electrochemical interface (1287, Solartron Analytical). The AC perturbation signal was 10 mV, and the frequency range was from 10^{-2} to 10^6 Hz in the EIS.

Solid-state rechargeable lithium batteries were fabricated with the $70\text{Li}_2\text{S}-30\text{P}_2\text{S}_5$ glass ceramic as the solid electrolyte and artificial graphite (SFG75, Timcal) as the anode material in place of thio-LISICON and the In–Li alloy in the electrochemical cell described above. The glass ceramic and the graphite were mixed in a weight ratio of 3:7, and 5.1 mg of the mixture was used as the anodes. The uncoated LiCoO_2 and sample 5 were used for the cathodes. The batteries were charged to 4.2 V at $63.7 \mu\text{A cm}^{-2}$ and then discharged down to 2 V at various current densities.

Received: December 5, 2005

Final version: May 25, 2006

- [1] B. Scrosati, *Nature* **1995**, 373, 557.
- [2] K. Takada, T. Inada, A. Kajiyama, H. Sasaki, S. Kondo, M. Watanabe, M. Murayama, R. Kanno, *Solid State Ionics* **2003**, 158, 269.
- [3] Y. Seino, K. Takada, B.-C. Kim, L.-Q. Zhang, N. Ohta, H. Wada, M. Osada, T. Sasaki, *Solid State Ionics* **2005**, 176, 2389.
- [4] R. Kanno, M. Murayama, *J. Electrochem. Soc.* **2001**, 148, A742.
- [5] F. Mizuno, A. Hayashi, K. Tadanaga, M. Tatsumisago, *Adv. Mater.* **2005**, 17, 918.
- [6] a) J. Maier, *Nat. Mater.* **2005**, 4, 805. b) J. Maier, *Prog. Solid State Chem.* **1995**, 23, 171.
- [7] C. C. Liang, *J. Electrochem. Soc.* **1973**, 120, 1289.
- [8] N. Sata, K. Eberman, K. Eberl, J. Maier, *Nature* **2000**, 408, 946.
- [9] J. B. Bates, N. J. Dudney, B. Neudecker, A. Ueda, C. D. Evans, *Solid State Ionics* **2000**, 135, 33.
- [10] P. G. Bruce, *Chem. Commun.* **1997**, 1817.
- [11] J.-M. Tarascon, M. Armand, *Nature* **2001**, 414, 359.
- [12] T. Ohzuku, A. Ueda, N. Yamamoto, *J. Electrochem. Soc.* **1995**, 142, 1431.
- [13] S. Takai, M. Kamata, S. Fujine, K. Yoneda, K. Kanda, T. Esaka, *Solid State Ionics* **1999**, 123, 165.
- [14] R. Moshtev, M. W. Carlen, *J. Power Sources* **2000**, 91, 210.
- [15] M. Winter, J. O. Besenhard, M. E. Spahr, P. Novak, *Adv. Mater.* **1998**, 10, 725.
- [16] R. Mosthev, B. Johnson, *J. Power Sources* **2000**, 91, 86.
- [17] W. D. Johnston, R. R. Heikes, D. Sestrich, *J. Phys. Chem. Solids* **1958**, 7, 1.
- [18] L. Aldon, P. Kubiak, M. Womes, J. C. Jumas, J. Olivier-Fourcade, J. L. Tirado, J. I. Corredor, C. P. Vicente, *Chem. Mater.* **2004**, 16, 5721.
- [19] K. Takada, N. Aotani, K. Iwamoto, S. Kondo, *Solid State Ionics* **1996**, 86–88, 877.